METHOD FOR CALCULATING PERFORMANCE CHARACTERISTICS OF HYDROKINETIC TURBINES

ADAM GÓRALCZYK, PATRYK CHAJA
AND ADAM ADAMKOWSKI

The Szewalski Institute of Fluid-Flow Machinery,
Polish Academy of Sciences,
Fiszera 14, 80-952 Gdansk, Poland
adam.goralczyk@gmail.com

(Received 23 January 2011; revised manuscript received 5 February 2011)

Abstract: This paper presents a numerical algorithm and its computer implementation (program) developed to determine the operational characteristics of axial flow hydrokinetic turbines. The program is based on the Vortex-Lattice Method (VLM), which proved useful for predicting hydrodynamic characteristics of screw propellers. In order to validate the software, we carried out a series of experiments on a laboratory test stand at the Institute of Fluid-Flow Machinery at the Polish Academy of Sciences (IMP PAN) in Gdansk. From the practical point of view, the agreement between the calculated and experimental results was satisfactory. Therefore, the developed numerical method can be a useful tool for the analysis of operating conditions and in the design of hydrokinetic turbines.

Keywords: Vortex-Lattice Method, performance characteristics, hydrokinetic turbines

Notation

B – free term
C – chord length of the runner blade profile
C_E – flow energy utilization rate
Cp – non-dimensional pressure coefficient
Cp_s – non-dimensional pressure coefficient on the suction surface of runner blade
Cp_p – non-dimensional pressure coefficient on the pressure face of runner blade
Cd – profile drag coefficient
D – turbine runner diameter
J – non-dimensional advance ratio
K_T – non-dimensional thrust coefficient
K_M – non-dimensional moment coefficient
m – number of vortices
n – axial speed of turbine runner
n – component of a vector normal to runner blade surface

$\vec{n}$ – unit vector normal to the surface at a control point
p_∞ – pressure in undisturbed flow
p – pressure at a control point
r – component of vector connecting the axis of rotation with a control point
$\vec{R}$ – vector connecting a control point with the runner axis of rotation
S – runner blade surface area
t – component of a vector tangent to runner blade surface
$\vec{t}$ – unit-length vector tangent to the surfaces of body elements at the i^{th} control point
V_n – value of velocity component normal to the surface at considered control point
V_s – value of velocity component tangent to the surface at considered control point
$\vec{V}_\infty$ – velocity vector in the undisturbed zone
$\vec{V}_\Gamma$ – vortex-induced velocity vector
$\vec{V}_r$ – relative velocity vector
W – influence coefficient
Δx – width of surface element, where bound vortex is placed
α – angle of attack of a blade profile
Γ – value of horseshoe vortex circulation
ϱ – liquid density
$\vec{\omega}$ – angular runner velocity
i – index of a control point
j – index of a horseshoe vortex
x – coordinate in the x-direction
y – coordinate in the y-direction
z – coordinate in the z-direction
Z – number of runner blades

1. Introduction

In the 1970s the Institute of Fluid-Flow Machinery at the Polish Academy of Sciences (IMP PAN) began working on software based on vortex methods in order to design and analyse the operation of screw propellers [1–5]. Since the designed software turned out to be a very precise and computationally efficient tool, it was applied to other turbo-machines, such as pumps [6] and mixers [7]. Nowadays, the work on developing software for determining the operating characteristics of the so-called hydrokinetic turbines, in the form of a system composed of a runner and housing (nozzle), continues. Such turbines are often applied to the recovery of the energy of sea tides and the kinetic energy of rivers.

The calculation method presented in this paper constitutes an extension of a previous method for determining the characteristics of screw propellers. The extension concerns not exactly the method but the application of the VLM to complex flow system of hydrokinetic turbine. In previous studies, each element of the "screw propeller-nozzle" (system) was treated separately in the calculation, and the influence of the nozzle on the operation of the screw was considered through subsequent approximations [2, 3].

In order to validate the developed software, the authors carried out experiments with models of three hydrokinetic turbines. The experiments were performed in a water tunnel at the IMP PAN in Gdansk. To drastically reduce the cost of research, the authors used the models of screw propellers and the co-operating nozzle already prepared at the IMP PAN. The main dimensions of the chosen runners and nozzle are presented further in the paper.

2. Calculation method

The physical model of a hydrokinetic turbine assumed in the calculation consisted of a runner with profiled blades, a hub and a housing, hereinafter referred to as nozzle (Figure 1).

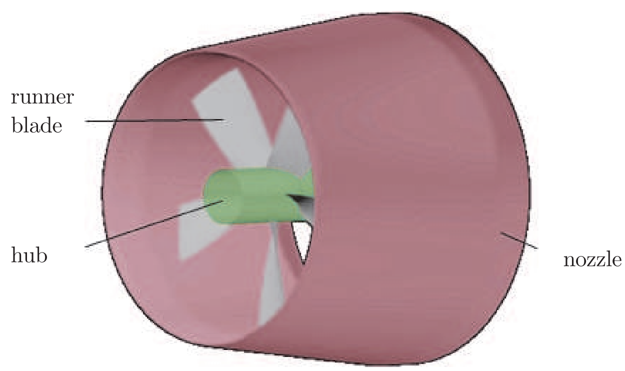

Figure 1. Assumed physical model of the hydrokinetic turbine

The calculation method developed for solving the problems of flow analysis of the given hydrokinetic turbine model is based on the Vortex-Lattice Method, a method based on a surface singularity distribution [8]. In this method, the irrotational flow of incompressible and inviscid liquid is assumed to be axisymmetric in the entire flow region, with the exception of singularities. In the case of flow through the considered turbine, the singular areas are the boundary layer of the elements (nozzle, runner blades, hub) and the vortex trace that forms behind those elements. These areas are characterized by a strong vortex concentration, which results mainly from friction forces [6]. The method is based on the discrete distribution of so-called horseshoe vortices in singular regions [8]. Such vortices can be either bound or free (Figure 2). In this way, a continuous vorticity distribution is replaced by a discrete distribution of whirl filaments, which are assumed to satisfactorily approximate the velocity field in the boundary layer and in its outer region. Subsequently, free vortices flowing off the trailing edge, approximate the vortex trace formed behind the elements of the turbine.

The first step in the flow analysis as performed using this method is the determination of the velocity field. The calculated field is the sum of the velocities of the undisturbed flow and the flow induced by vortex layers. Subsequently, the pressure field is determined on the basis of the Bernoulli equation.

The method neglects the turbulent motion and other phenomena resulting from the liquid viscosity, *e.g.* flow separation. Simultaneously, it was assumed that the surface vortex distribution for large Reynolds numbers satisfactorily approximates the velocity field in the boundary layer.

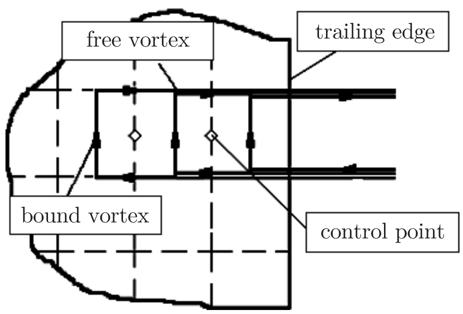

Figure 2. Diagram of the calculation mesh showing discrete whirl filaments

The second step in solving the problem is to determine the circulation Γ of vortex filaments given on the surfaces of the flow elements of the analyzed system. In order to achieve this, the authors apply the Neumann condition by setting the velocity in the direction normal to the surface of the body to 0, which can be expressed as follows:

$$V_{ni}=\vec{V}_{ri}\cdot\vec{n}_i+\vec{V}_\Gamma\cdot\vec{n}_i=0 \tag{1}$$

where V_{ni} denotes the magnitude of the velocity normal to the surface at the i^{th} control point, $\vec{V}_{ri}$ is the relative velocity vector, $\vec{V}_\Gamma$ is the velocity induced by vortices, $\vec{n}_i$ is the vector normal to the surface at the i^{th} control point.

The velocity $\vec{V}_\Gamma$ was determined from the Biot-Savart formula, which can be written in the form:

$$\vec{V}_\Gamma=\sum_{j=1}^{m}\Gamma_j\left(\frac{1}{4\pi}\int_l\frac{\vec{r}_{ij}\times d\vec{l}}{r_{ij}^3}\right) \tag{2}$$

Subscripts i and j index the control points and horseshoe vortices, respectively.

After applying the above relation to all control points on the surfaces of the flow elements of the turbine, the following system of linear equations is obtained:

$$\Gamma_j W_{ij}=B_i \tag{3}$$

W_{ij} is the influence coefficient of the j^{th} horseshoe vortex on the i^{th} control point, and is calculated from the relationship:

$$W_{ij}=\left(\frac{1}{4\pi}\int_l\frac{\vec{r}_{ij}\times d\vec{l}}{r_{ij}^3}\right)\cdot\vec{n}_i \tag{4}$$

where Γ_j is the unknown value of the circulation of the j^{th} horseshoe vortex, B_i is a free term calculated as:

$$B_i=-\vec{V}_{ri}\cdot\vec{n}_i \tag{5}$$

– in the case of non-rotating turbine elements (corresponding to the nozzle):

$$\vec{V}_{ri} = \vec{V}_{\infty} \tag{6}$$

– in the case of rotating elements (corresponding to the rotor and hub):

$$\vec{V}_{ri} = \vec{V}_{\infty} + \vec{\omega} \times \vec{R}_i \tag{7}$$

where $\vec{V}_{\infty}$ denotes the velocity in the undisturbed zone, $\vec{V}_{ri}$ is the relative velocity, $\vec{\omega}$ is the rotor angular velocity, $\vec{R}_i$ is a vector connecting the i^{th} control point with its axis of rotation.

The obtained system of equations (3) is not closed, because the number of vortices is larger than the number of control points (see Figure 3). In order to close this system of equations, the authors invoke the Kutta-Joukowski theorem. It assumes the equilibrium of pressure on both sides of the blade at the trailing edge, which is true on condition that the circulation of the bound vortex at the trailing edge is equal to 0. The equations necessary to close the system (3) were obtained by linear interpolation of circulation distribution related to the chord length:

$$\frac{\Gamma_N - \Gamma_C}{X_N - C} = \frac{\Gamma_{N-1} - \Gamma_C}{X_{N-1} - C} \tag{8}$$

Putting into the Equation (8) $\Gamma_C = 0$, for selected calculation grid, one has been obtained:

$$-\frac{1}{3}\Gamma_{N-1} + \Gamma_N = 0 \tag{9}$$

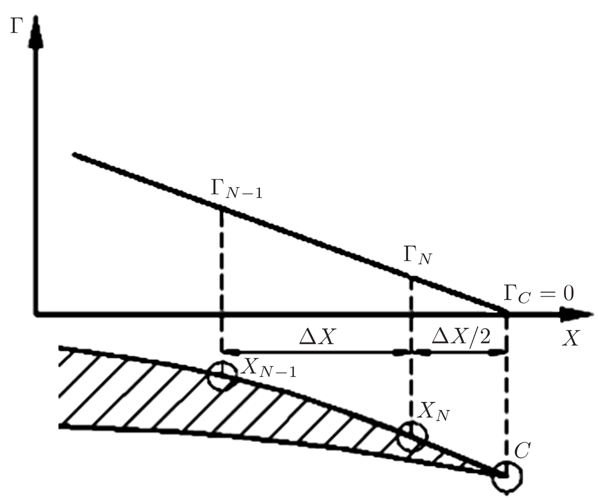

Figure 3. Linear circulation distribution in the region close to the profile edge, assumed according to the Kutta-Joukowski condition (N denotes the number of vortices distributed along the chord of the profile)

After having determined the circulation of horseshoe vortices, the values of the velocities tangent to the walls of the analyzed flow elements are calculated from the following relationship:

$$V_{si} = \sum_{j=1}^{m} WS_{ij}\Gamma_j + \vec{V}_{ri}\cdot\vec{t}_i \pm \frac{\Gamma_i}{2\Delta x_i} \tag{10}$$

where

$$WS_{ij} = \frac{1}{4\pi}\int_l \frac{\vec{r}_{ij}\times d\vec{l}}{r_{ij}^3}\cdot\vec{t}_i \tag{11}$$

where $\vec{t}_i$ is a unit vector tangent to the surfaces of the body elements at the i^{th} control point, Δx_i is the width of the surface element, where the bound vortex is located, "+" refers to the suction surface of the rotor blade, hub surface and the nozzle, whereas "−" refers to the pressure face of the rotor blade.

Basing on the Bernoulli equation, the values of the non-dimensional pressure coefficient for the obtained tangent velocities are computed from:

$$Cp_i^* = \frac{p_\infty - p_i}{\frac{1}{2}\rho V_{ri}^2} = 1 - \frac{V_{si}^2}{V_{ri}^2} \tag{12}$$

where p_∞ denotes the pressure in undisturbed flow, p_i is the pressure at the i^{th} control point, ρ is the liquid density.

The non-dimensional pressure coefficient Cp_i needs to be evaluated only on the surfaces of turbine runner blades. Owing to the thin profiles of the blades, the values of this coefficient are determined on the profile mean lines. This simplification leads to a singularity in the pressure at the leading edge. The singularity can be avoided by applying, as in previous studies [1, 6], the so-called correction for the radius of the profile curvature, by introducing a correction factor expressed as:

$$Cpr_i = \frac{x_i}{x_i + 0.5r} \tag{13}$$

where x_i is the non-dimensional coordinate of the profile length, r is the non-dimensional radius of the curvature of the profile edge of attack.

Finally, the following relationship is obtained for the calculation of the non-dimensional pressure coefficient:

$$Cp_i = Cp_i^* \, Cpr_i \tag{14}$$

The resulting distribution of the non-dimensional pressure coefficient is further used in order to compute the value of the torque M of the turbine rotor and its axial thrust force T. These values are determined from the integral relationships given below:

$$M = \frac{1}{2}\rho\int_S V_r^2\left[(Cp_s - Cp_p)(n_Y\cdot r_Z - n_Z\cdot r_Y) + Cd(t_Y r_Z - t_Z r_Y)\right]ds \tag{15}$$

$$T = \frac{1}{2}\rho\int_S V_r^2\left[(Cp_s - Cp_p)n_X + Cdt_X\right]ds \tag{16}$$

where S is the surface area of the runner blade, r_z, r_Y are the components of the vector connecting the axis of rotation with the control point, t_x, t_y, t_z are the components of the vectors tangent to the runner blade surface, n_x, n_y, n_z are the components of the vectors normal to the runner blade surface, Cp_s is the non-dimensional pressure coefficient on the drag surface of the runner blade, Cp_p is the non-dimensional pressure coefficient on the pressure face of the runner blade, Cd is the profile drag coefficient given as [1, 3]:

$$Cd = Cd_0 + 0.001(\alpha - 1)^2 \tag{17}$$

where $Cd_0 = 0.011$ is the value obtained from the model test of the blade profile and α is the angle of attack of the blade (in degrees).

Basing on the resulting values of M and T, the non-dimensional coefficients of the moment K_M, thrust K_T and the energy utilization rate of the liquid stream C_E can be determined. The coefficients are defined by following formulae:

- moment coefficient

$$K_M = \frac{M}{\rho n^2 D^5} \tag{18}$$

- thrust coefficient

$$K_T = \frac{T}{\rho n^2 D^4} \tag{19}$$

- flow energy utilization rate

$$C_E = \frac{2\pi n M}{0.5\rho V_\infty^3 0.25\pi D^2} = 16\frac{K_M}{J^3} \tag{20}$$

where n denotes the turbine runner speed of rotation (1/s), D is the runner diameter, J is the advance ratio determined by:

$$J = \frac{V_\infty}{nD} \tag{21}$$

The flow energy utilization rate defined as the ratio of the energy generated by the turbine to the kinetic energy of the liquid flow is equivalent to the energy efficiency of hydraulic turbines utilizing the potential energy of the liquid column.

The calculation algorithm presented above was the basis for preparation of the computer program.

3. Modelling studies

Experiments with turbine models were carried out in a water tunnel extensively used for the hydrodynamic research of propeller models since 1960. A photograph of the test stand is presented in Figure 4, and its scheme – in Figure 5. The experimental chamber of the test rig had a square cross section of $0.425 \times 0.425\,\mathrm{m}^2$. A circulating pump allowed us to perform measurements with the maximum average water flow velocity in the chamber of up to 5m/s.

The test stand equipment allowed us to measure the angular velocity of the turbine runner (wheel), average water flow velocity in the tunnel chamber,

Figure 4. Water tunnel of the test rig

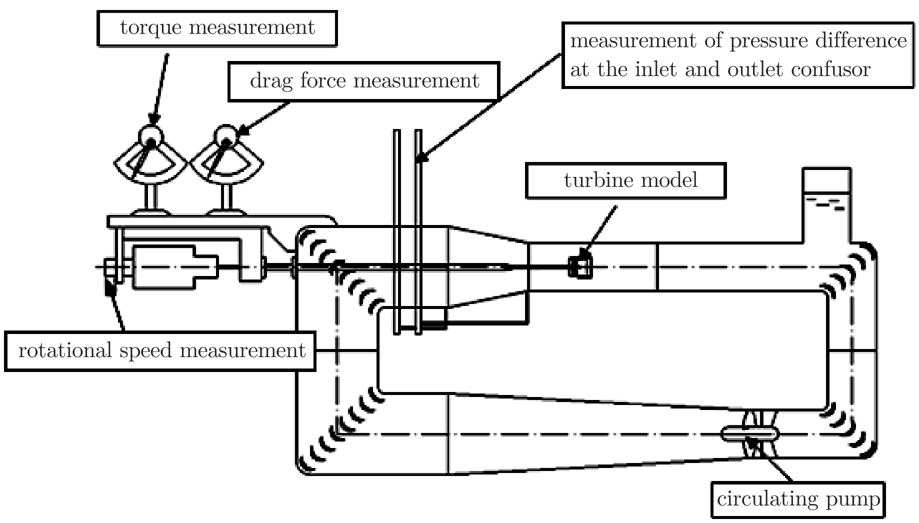

Figure 5. Schematic of the test stand

the turbine output torque and the axial force induced by the considered turbine runner model.

To measure the rotational speed of the runner, we used the counter of impulses generated by a slotted catch plate.

Measurements of the average water velocity in the chamber (V_∞) were processed indirectly using a calibrated tunnel confusor. To achieve this, the difference between the height of the water columns at the inlet and outlet cross sections of the tunnel confusor (ΔH) was measured with a precise differential manometer, and the average water velocity was calculated on the basis of the relationship $V_\infty = f(\Delta H)$, derived from the calibration. The estimated accuracy of the measurements of the average velocity was ± 0.036 m/s.

The torque at the shaft of the model was measured *in situ* with a tangent balance. In order to eliminate the influence of the friction forces on the model turbine shaft (and in its bearing pairs in particular), additional measurements were performed. The measurements consisted in the experimental determination of torque of shaft friction forces as a function of rotational speed when the turbine runner was disassembled. The torque measured during the turbine model tests was corrected with regard to the value of torque of shaft friction forces obtained at the considered rotational speed. The measurement uncertainty of the torque was estimated to be ± 0.01 Nm.

The force of hydraulic flow pressure generated by the runner was measured using a dynamometer in the form of a tangent balance. Its measurement uncertainty was estimated to be ± 0.98 N.

The systematic uncertainties of the experimentally determined values of non-dimensional coefficients of torque, axial flow pressure and advance were calculated by computing the total derivatives of the function describing the non-dimensional coefficients K_M, K_T, C_E and J to be determined. The values of these uncertainties are denoted in the figures presented further in the paper.

Three turbine models with identical runner diameters, $D = 148$ mm, and different values of the blade pitch h/D and its Z number were considered:

- $h/D = 1.0$, $Z = 5$ (**model 1**);
- $h/D = 1.0$, $Z = 4$ (**model 2**);
- $h/D = 1.2$, $Z = 4$ (**model 3**).

The models also differed with respect to the chord length and the thickness of the blade profile (*cf.* table in Figure 6). Selected runners were tested in cooperation with the nozzle. The simplified geometry of the investigated runners and of the nozzle is presented in Figures 6–7. In each model, the runner was placed at a distance of 35 mm, measured from the inlet cross section of the nozzle to the front surface of the runner hub.

Experiments with each turbine model were performed using similar conditions of the water flow in the tunnel. During the measurements, the average flow velocity in the water tunnel was kept constant at 3.25 m/s with a tolerance of ± 0.05 m/s. A change in the operation parameters of the studied turbine model under these conditions was obtained by varying the load of the turbine-driven generator. This resulted in the change in the axial velocity of the runner.

On the basis of the tests, we determined the non-dimensional coefficients K_M, K_T, C_E and J, defined by Formulae (18)–(21). The results of the performed investigations are presented in Figures 8–10 and are compared with the results obtained using the developed program.

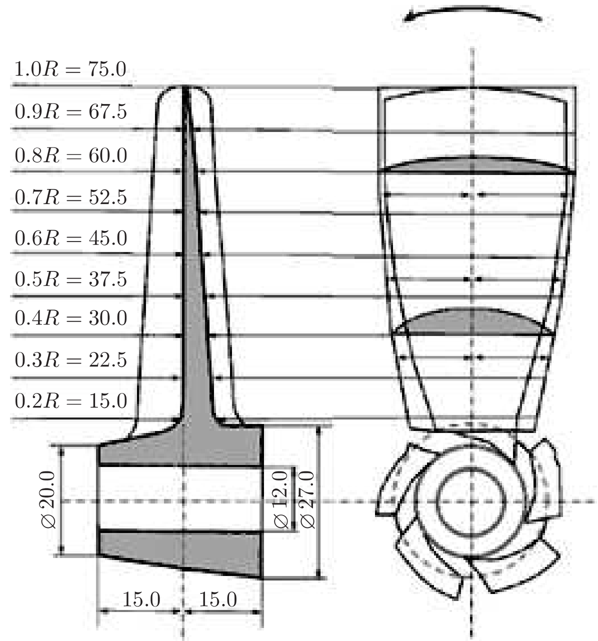

Distance from the runner axis	$Z=5$, $h/D=1$ (model 1)		$Z=4$, $h/D=1$ (model 2)		$Z=4$, $h/D=1.2$ (model 3)	
	C [mm]	t [mm]	C [mm]	t [mm]	C [mm]	t [mm]
R	33.2	1.3	32.5	0.8	30.5	0.7
$0.9R$	33.2	1.9	32.2	1.5	30.2	1.4
$0.8R$	32.5	2.4	31.4	2.1	29.4	1.9
$0.7R$	31.1	2.9	30.0	2.6	28.1	2.5
$0.6R$	29.3	3.4	28.6	3.2	26.8	3.0
$0.5R$	27.2	4.0	26.8	3.8	25.1	3.5
$0.4R$	25.1	4.5	25.0	4.3	23.4	4.0
$0.3R$	23.2	5.0	23.5	4.7	22.0	4.3
$0.2R$	21.6	5.5	22.2	5.5	20.8	5.1

Figure 6. Geometry of the runners including the chord length distribution (C) and the maximum profile thickness (t) of the given radial cross sections

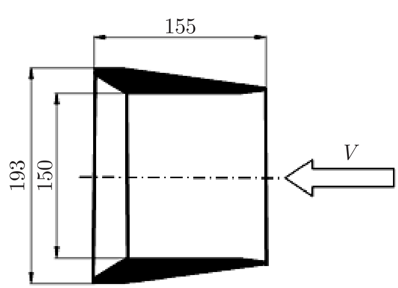

Figure 7. Geometry of the nozzle

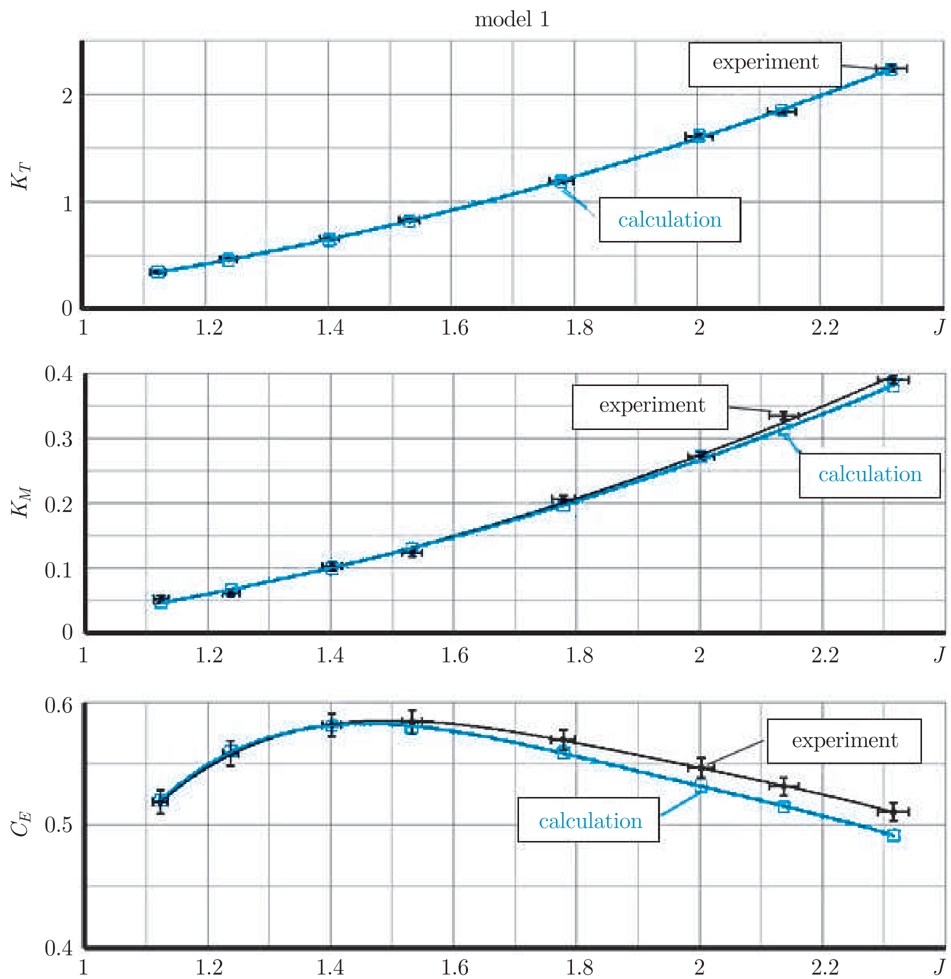

Figure 8. Comparison of experimental results and the predictions for the turbine model 1 (number of blades $Z=5$, blade pitch $h/D=1$)

4. Calculated results and their comparison with the results of laboratory measurements

The calculations of flow parameters by means of the above models of hydrokinetic turbines and non-dimensional coefficients were performed using the aforementioned program after the experimental tests of these models. The measured runner axial velocities of the investigated models and the average velocities in the tunnel chamber were taken for the calculations and treated as the values for undisturbed and homogeneous flow. Thus, the authors neglected the actual effect of the tunnel walls on the liquid flow velocity distribution resulting from the forces of friction. Hence, the liquid flow velocities assumed in the calculations were lower than the actual inflow velocities of the studied turbine models. From [9] it follows that during the tests of marine propellers of

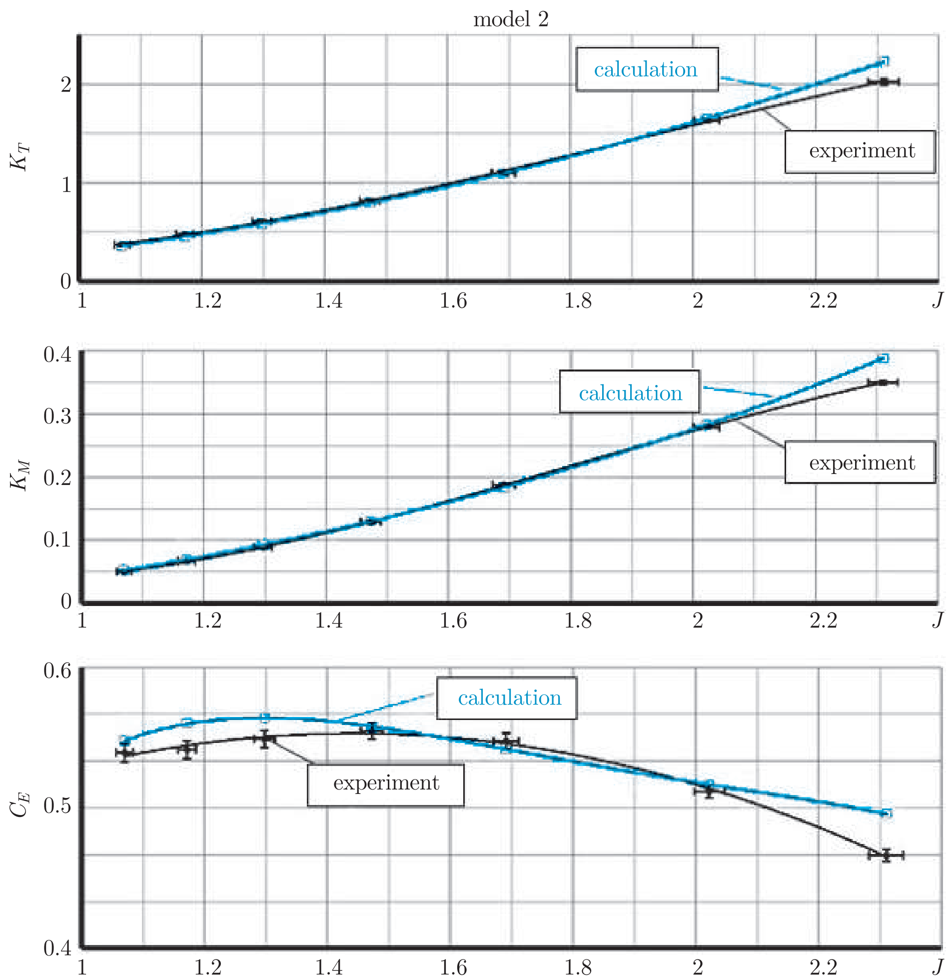

Figure 9. Comparison of experimental results and the predictions for the turbine model 2 (number of blades $Z=4$, blade pitch $h/D=1$)

similar dimensions, which were carried out on the test stand described earlier, the influence of the flow tunnel walls on the hydrodynamic characteristics of these models was estimated to be 2–3% of torque values.

Figures 8–10 present the comparison of the computed results and laboratory measurements in the non-dimensional coordinates defined above, *i.e.* $J-K_T$, $J-K_T$ and $J-C_E$. Numerical and experimental results were denoted as points, while the least-squares fits of the results were denoted with lines. The figures demonstrate good agreement between the experimental data and the calculated results obtained by means of the developed numerical method. In the vicinity of the optimum operating points of the investigated turbine models (*i.e.* in the regions characterized by the maximum flow energy utilization rate C_E), the relative differences between the calculated and experimental values of the coefficients

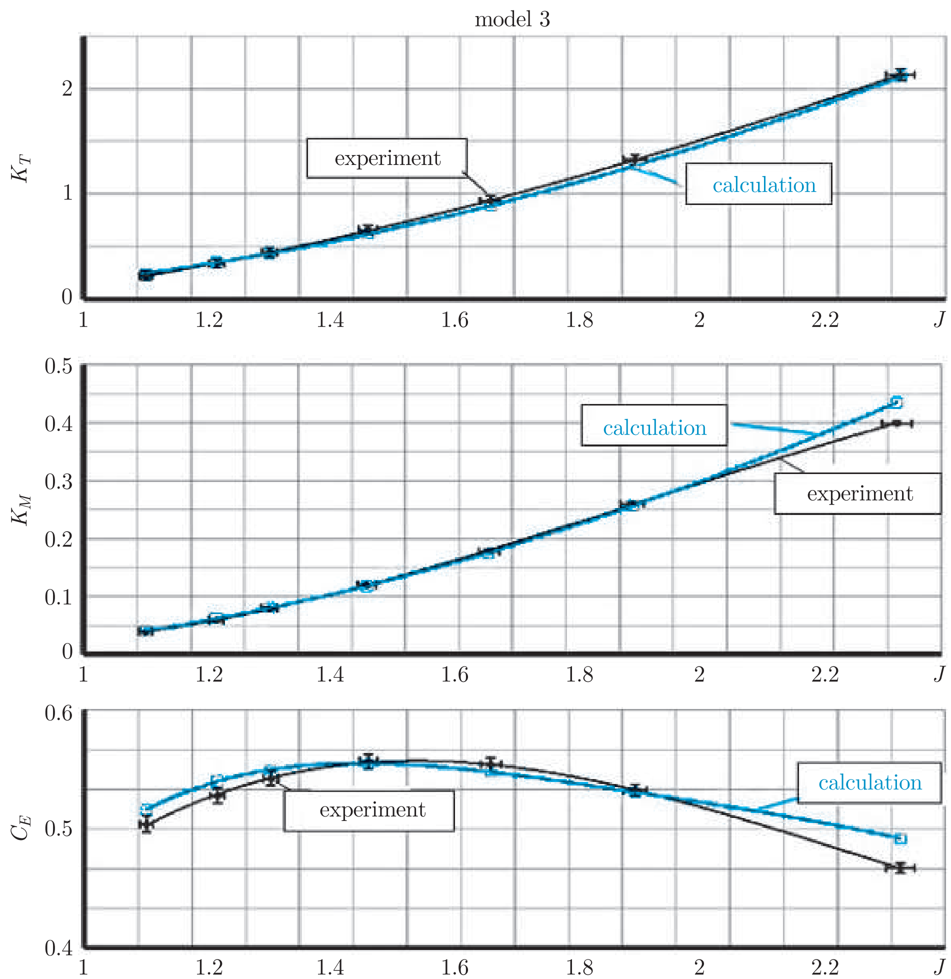

Figure 10. Comparison of experimental results and the predictions for the turbine model 3 (number of blades $Z = 4$, blade pitch $h/D = 1.2$)

K_T, K_M and C_E did not exceed 5%, and for several points lay within the range of measurement uncertainty (1.5–2.5%). In each case, the largest difference between the calculated and experimental values of the coefficients was observed for the highest value of the advance ratio J, where the relative difference between the calculated and experimental coefficients K_M and C_E exceeded 10%. We also observed increasing disagreement between the calculations and experiment for the smallest values of the advance ratio J. We attribute this to the neglect of the viscous flow separation in the computation algorithm.

The effect of the actual tunnel wall, neglected in the calculations, could have led to a considerable increase in the flow energy utilization rate and in the torque coefficient (the inflow velocity was higher for the considered runners, as compared with the measured average velocity).

The energy utilization rate for the five-blade runner was higher than for the four-blade runner. Moreover, regarding previous research on this type of runners without the nozzle [10], the nozzle effect was beneficial, since it increased the flow energy utilization rate. However, the shape of the nozzle was not optimum for cooperation with the turbine runners. Therefore, shape optimization calculations and additional measurements with another nozzle may be necessary.

5. Conclusions

The authors developed an algorithm based on the vortex-lattice method and implemented it in a computer code for the calculation of the operating characteristics of hydrokinetic turbines, accounting for the full three-dimensional geometry of the machinery. From the engineering point of view, the authors achieved satisfactory agreement between the values of the non-dimensional coefficients calculated with our program and the corresponding values obtained from laboratory measurements of three turbine models and for a wide range of loads. In general, the differences between these values did not exceed several percent for the operating conditions of the investigated models that do not depart considerably from their working points, for which the flow energy utilization rate reached maximum. The largest discrepancies between the calculated and experimental values of the energy utilization rate, reaching several percent, were observed for the highest values of the advance ratio J. We presume that the discrepancies resulted from the simplifications inherent in the computational method, from the fact that the effect of the tunnel wall was neglected in the test results, and from the neglect of viscous flow separation. In practical terms, the developed computer program can be a useful tool for the analysis of the operating conditions and design of hydrokinetic turbines.

Acknowledgements

This work was conducted as part of the statutory activities of IMP PAN in Gdansk under the research project "Agro-energy complexes as an example of dispersed co-generation based on local renewable energy sources" (No. POIG. 01.01.02-00-016/08).

References

[1] Jarzyna H, Koronowicz T and Szantyr J 1996 *Design of Marine Propellers*, Maszyny Przepływowe, Ossolineum, **20**

[2] Szantyr J A 1988 *User Manual for the DUNCAN Program for the Analysis of Ducted Propellers in Non-Uniform Velocity Field*, Report of the IMP PAN No. 150, Gdansk (in Polish)

[3] Wilczyński L 1992 *A Computer Algorithm for Calculation of Hydrodynamical Characteristics of Ducted Propellers*, Report of the IMP PAN No. 361/1323, Gdansk

[4] Koronowicz T, Tuszkowska T, Waberska G, Krzemianowski Z, Chaja P and Góralczyk A 1996 *Design Algorithm for Screw Propellers*, Report of the IMP PAN No. 6103, Gdansk (in Polish)

[5] Koronowicz T, Krzemianowski Z, Tuszkowska T and Góralczyk A 1998 *System of Programs for the Design of Ducted Propellers*, Report of the IMP PAN No. 345, Gdansk (in Polish)
[6] Kaniecki M 2004 *Hydrodynamic Analysis of Axial Pumps Performance Using Vortex Lattice Method*, PhD Thesis, IMP PAN, Gdansk (in Polish)
[7] Koronowicz T 2008 *The Results of Design Calculations of* $D = 1.34\,m$ *Mixers Series*, Report of the IMP PAN, Gdansk (in Polish)
[8] Lewis R I 1991 *Vortex Element Methods for Fluid Dynamic Analysis of Engineering Systems*, Cambridge University Press
[9] Koronowicz T 1965 *Influence of the Measurement Segment Walls of the Cavitation Channel for Marine Propellers Performances*, PhD Thesis, IMP PAN, Gdansk (in Polish)
[10] Góralczyk A, Chaja P and Koronowicz T 2010 *TASK Quart.* **14** (3) 311